IGNITION CONDITIONS FOR PERIPHERAL PLASMA IN A GROUNDED CHAMBER CONNECTED TO A DUAL FREQUENCY CAPACITIVE DISCHARGE

by

M. A. Lieberman, A. J. Lichtenberg, Sungjin Kim
and J. T. Gudmundsson

Memorandum No. UCB/ERL M05/10

12 March 2005

IGNITION CONDITIONS FOR PERIPHERAL PLASMA IN A GROUNDED CHAMBER CONNECTED TO A DUAL FREQUENCY CAPACITIVE DISCHARGE

by

M. A. Lieberman, A. J. Lichtenberg, Sungjin Kim
and J. T. Gudmundsson

Memorandum No. UCB/ERL M05/10

12 March 2005

ELECTRONICS RESEARCH LABORATORY

College of Engineering
University of California, Berkeley
94720

IGNITION CONDITIONS FOR PERIPHERAL PLASMA IN A GROUNDED CHAMBER CONNECTED TO A DUAL FREQUENCY CAPACITIVE DISCHARGE

M. A. Lieberman, A. J. Lichtenberg, and Sungjin Kim
Department of Electrical Engineering and Computer Sciences - 1770
University of California, Berkeley CA 94720
and
J. T. Gudmundsson
Science Institute, University of Iceland, Dunhaga 3, IS-107, Reykjavik, Iceland
and Department of Electrical and Computer Engineering
University of Iceland, Hjardarhaga, 2-6, IS-107 Reykjavik, Iceland

March 12, 2005

ABSTRACT

A configuration of both theoretical and practical interest is a capacitive discharge connected through a slot to a peripheral grounded pumping region. The configuration is used in commercial dual frequency capacitive discharges with one frequency higher than the usual industrial frequency of 13.56 MHz, with application to dielectric etching on large area substrates. In some configurations a dielectric slot surrounding the substrate separates the main plasma from a peripheral pumping region. Ignition of the peripheral plasma produces detrimental effects on processing performance. Discharge models for diffusion and plasma maintenance in the slot have been developed to obtain conditions for ignition of a plasma in the periphery. An experiment has been constructed at Berkeley to compare with and validate theoretical predictions of ignition conditions.

I. INTRODUCTION

The transport and maintenance of rf-generated plasma in gaps, slots, or tubes is both of physical interest and can have important technological implications. The particular configuration of interest for this study, shown schematically in Fig. 1, is a dual frequency capacitive discharge, with the main discharge connected to a peripheral (pumping) region through an annular dielectric slot. The feedstock gas flows from the main discharge region through the slot, and is pumped in the grounded peripheral chamber. In operation of a commercial reactor, a peripheral plasma is found to produce detrimental effects on processing. This study is designed to understand the conditions for which peripheral ignition occurs, and therefore to determine the conditions required to confine the discharge to the central region. As shown in the figure, the discharge is driven by a high frequency source of frequency ω and voltage $V_{\rm rf}$ in series with a low frequency source of frequency ω_b and voltage $V_{\rm bias}$. The main discharge, having plate separation l, is connected to a peripheral region of length $w_{\rm per}$ through an annular dielectric slot of length w and gap g. Because of the small pumping conductance of the slot, there can be a significant pressure gradient within the slot. We do not consider the slot pressure gradient in this study, but we do allow for different average pressures in the slot and peripheral regions. The configuration in the figure is based on a commercial reactor, but the particular dimensions used are related to a research experiment that has been built to study the phenomena. We use nominal parameters $l = 3$ cm, $g = 0.5$ cm, $w = 3$ cm and $w_{\rm per} = 3$ cm. We vary these parameters to determine their effect on ignition. To explore the critical parameter of the gap g, it is adjustable in the experiment, by varying the thicknesses of the dielectric (quartz) rings.

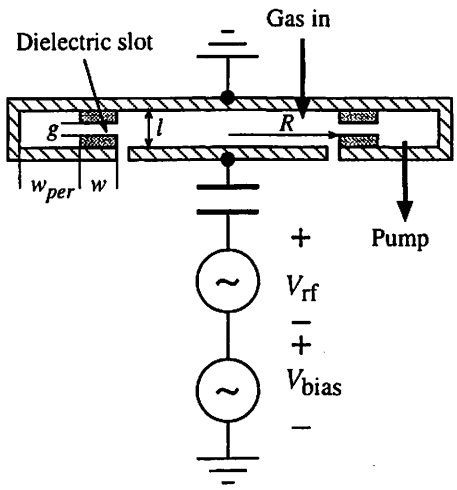

Figure 1. Confined plasma operation of a dual frequency capacitive discharge.

A number of important issues determine ignition of the peripheral plasma.

(1) Plasma transport in the slot. What conditions are required for the diffusion of plasma a particular distance from the main discharge into the slot and, perhaps, into the periphery? In Sec. II, we develop a model based on the following physics. The main discharge sets a uniform dc plasma potential in the slot

and a plasma density at the slot entrance. Typically, the dc potential can be hundreds of volts. Assuming diffusion of plasma into the slot and loss of plasma on the slot walls, then the density decays into the slot and the sheath thickness, determined by a Child law, increases. When the sheath thickness grows to be approximately half of the gap spacing, then the plasma "pinches off" inside the slot.

(2) Maintenance of a discharge. What conditions are required to maintain a discharge in the slot and in the periphery, either separately or together? In Sec. III, we determine the minimum rf voltage required to maintain a conventional planar (one-dimensional) discharge, depending on the pressure. At low pressures, with a small resistive voltage component, the maintenance voltage is determined by the condition that the total thickness of the sheaths approaches closely the gap spacing, leading to a thin bulk plasma. The sheath thickness becomes large at either very low or very high rf voltages, yielding a double-valued maintenance curve at a given pressure.

(3) Wave propagation, radial current flows, and voltage variations in the slot. Since the slot plasma is driven at one end (its inner radius) by the rf voltage of the main discharge plasma, with the top and bottom slot surfaces earthed through the quartz confinement rings, there is wave propagation and a large radial component of the rf current when a slot plasma is ignited. The radial current further increases when a peripheral plasma is also ignited, which draws its current through the slot. We determine the power absorption and the radial variation of the rf voltage under these conditions. When there is no slot plasma, the rf plasma voltage $\widetilde{V}_d$ of the main discharge capacitively couples through the slot to the periphery, which can ignite a peripheral plasma. In Sec. IV, we incorporate these two-dimensional effects into the maintenance models.

Figure 2 shows typical maintenance voltages versus pressure under various conditions, which determine the ignition of peripheral plasma as the high frequency plasma voltage $\widetilde{V}_d$ of the main discharge (and the plasma density) increases. For example, starting with a low voltage $\widetilde{V}_d \approx 10$ V at 50 mTorr (point X in Fig. 2a), the two solid curves give the maintenance conditions (ignition voltage versus pressure) for the periphery (with no plasma in the slot) and for the slot (with no plasma in the periphery). Since X lies below these curves, neither the slot nor the periphery ignite. Increasing the voltage to $\widetilde{V}_d \approx 100$ V (point Y) produces some plasma diffusion into the slot. The maintenance curve for the periphery then decreases (dashed curve) because the capacitive coupling across the slot increases. However, the periphery still does not ignite. As shown in Fig. 2b, upon increasing the voltage to $\widetilde{V}_d \approx 300$ V (point Z), above the maintenance curve for the slot (with no plasma in the periphery, shown here as a dot-dashed line), the slot ignites.

The ignited slot plasma connects the main discharge to the periphery, causing the maintenance curve for the periphery to decrease from high voltages (dashed line) to much lower voltages (solid line). At this time the peripheral plasma ignites, drawing its current through the slot, which causes the maintenance curve for the slot to shift (decreasing at 50 mTorr from the dashed to the solid curve).

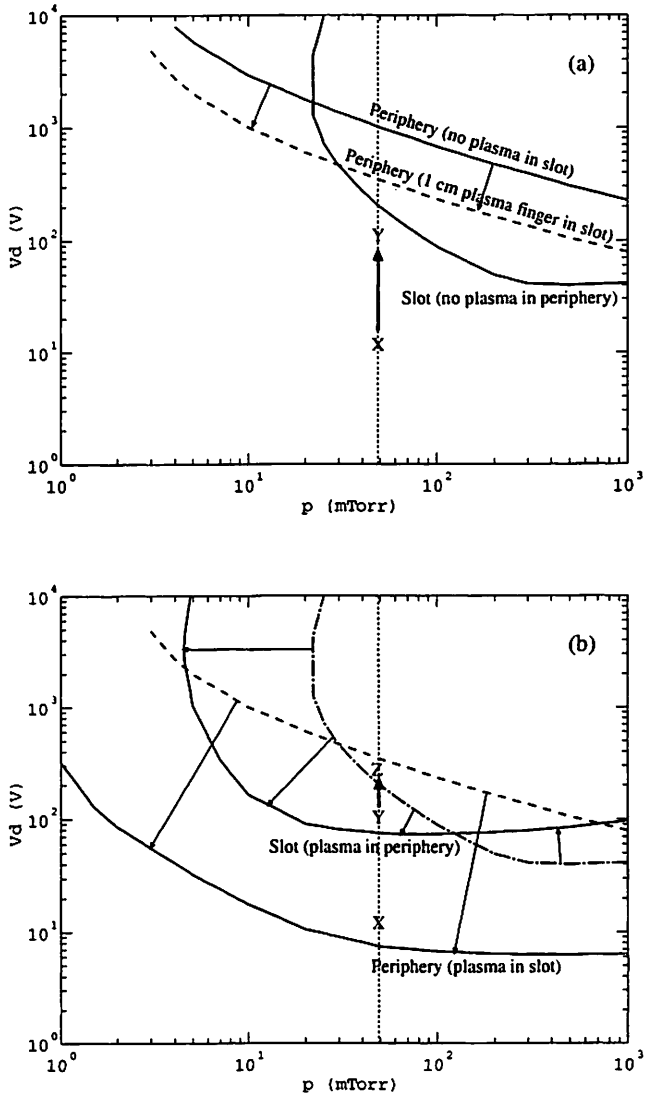

Figure 2. High frequency maintenance voltage $\widetilde{V}_d$ versus pressure p for various conditions, illustrating the loss of main discharge confinement as $\widetilde{V}_d$ increases.

In the final state for the loss of confinement shown in Fig. 2b, the voltage at point Z lies well above both maintenance curves (solid lines), indicating a considerable hysteresis in the characteristics. The voltage would have to be reduced to well below 100 V for confinement to be restored. Figure 2b also indicates a possible instability at higher pressures (above about 120 mTorr for these parameters), where the maintenance voltage for the slot increases rather than decreases when the periphery ignites. This is due to the increased

ohmic component of the voltage across the slot plasma at the higher pressures, a hysteresis effect which may leaad to instability. A second possible source of instability is a reduction in $\widetilde{V}_d$ itself when the peripheral plasma ignites, due to the increased grounded area seen by the plasma in the main discharge. In Sec. V, we give some measurements of the hysteresis and instabilities seen in our experiments. Conclusions and a discussion of future work are given in Sec. VI.

II. PLASMA TRANSPORT IN THE SLOT

The main discharge sets a uniform dc plasma potential $\overline{V}$ in the slot, and a plasma density n_0 at the slot entrance. Typically, $\overline{V}$ can be hundreds of volts. Assuming diffusion of plasma and plasma loss on the slot walls, then the density drops and the sheath thickness s, determined by a Child law, increases. When the sheath thickness grows to be approximately half of the gap spacing, $s \approx g/2$, then the plasma "pinches off" inside the slot.

To estimate the scaling of the plasma decay resulting in pinch-off in the slot we first use the simplest (high pressure) rectangular coordinate diffusion model, neglecting ionization in the slot, to obtain the diffusion equation

$$-D_a \nabla^2 n = 0 \tag{1}$$

where D_a is the ambipolar diffusion coefficient, $n(x,z)$ is the density in the slot, and x corresponds to the radial direction with $x = 0$ at the slot entrance. Taking $n = n_0$ at $x = 0$ and approximating $n = 0$ at $z = \pm g/2$, (1) has a fundamental diffusion mode solution

$$n = \frac{4\,n_0}{\pi} \cos\left(\frac{\pi z}{g}\right) \exp\left(-\frac{\pi x}{g}\right) \tag{2}$$

which gives a very short decay length $\Lambda = g/\pi$. We assume a collisionless Child law to determine the sheath thickness $s_{\rm slot}$:

$$e h_l n u_B = K_{\rm CL} \epsilon_0 \left(\frac{2e}{M}\right)^{1/2} \frac{\overline{V}^{3/2}}{s^2} \tag{3}$$

where h_l is an edge-to-center density ratio, $K_{\rm CL} \approx 0.82$ (see Table 1), and $u_B = (e\mathrm{T_e}/M)^{1/2}$ is the Bohm velocity. Examining first the configuration in which the confinement rings are grounded conductors, not dielectrics, the dc voltage across each sheath in the slot is

$$\overline{V} = K_{\rm v} \widetilde{V} + 4.8\,\mathrm{T_e} \tag{4}$$

where $K_{\rm v} \approx 0.82$ (see Table 1) and $\widetilde{V} = \widetilde{V}_d + \widetilde{V}_b$ is the total rf voltage across the sheath, with $\widetilde{V}_d$ and $\widetilde{V}_b$ the high and low frequency rf plasma voltages of the main discharge, respectively. The term $4.8\,\mathrm{T_e}$ gives a sheath thickness of approximately 3.5 Debye lengths when the rf voltages are near zero, and the factor $K_{\rm v}$ relates the rf voltages to the dc voltages. We take the condition for pinch-off that the two sheaths expand to fill the entire gap, $s = g/2$ at position $x = w_{\rm po}$. At $w_{\rm po}$, where the bulk plasma thickness within the slot

vanishes, we use the (collisionless) Langmuir solution for the diffusion to estimate $h_l = 0.425$ [1, p. 139]. Setting $x = w_{po}$ in (2) and $s = g/2$ in (3), we can eliminate n to obtain

$$0.135\, e n_0 \exp(-\pi w_{po}/g) g^2 = K_{CL}\epsilon_0 \left(\frac{2e}{M}\right)^{1/2} \overline{V}^{3/2} \tag{5}$$

Solving for w_{po}, we obtain

$$w_{po} = \frac{g}{\pi} \ln\left[\frac{0.135\, e}{K_{CL}\epsilon_0}\left(\frac{M}{2e}\right)^{1/2} \frac{n_e}{\overline{V}^{3/2}}\right] \tag{6}$$

with $\overline{V}$ given by (4). Equation (6) gives w_{po} as a function of the voltages, densities, and slot dimensions, and shows that the pinch-off length is proportional to the gap spacing g and depends weakly (logarithmically) on the other system parameters. For typical parameters $n_0 = 2 \times 10^{11}$ cm^{-3}, $\overline{V} = 100$ V, and $T_e = 2$ V (at 50 mTorr), we find a pinch-off length $w_{po} \approx 0.7$ cm for an 0.5 cm gap. The results for the decay of the plasma density into the slot are shown for the high pressure diffusion model as the dotted line in Fig. 3.

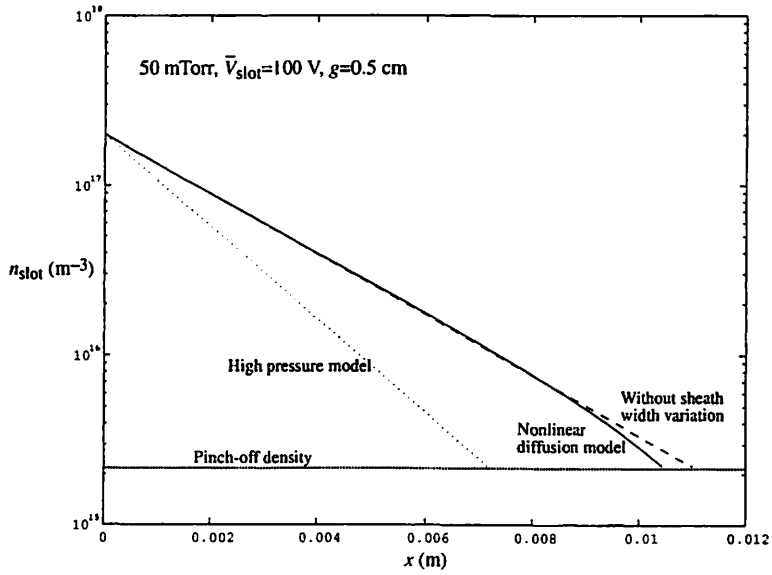

Figure 3. Plasma density in the slot versus position at 50 mTorr in argon, showing the pinch-off length w_{po} using various diffusion models.

Table 1. Coefficients for collisionless and collisional models

Coefficient	Collisionless Model	Collisional Model
K_{CL}	0.83	$1.68(\lambda_i/s_m)^{1/2}$
K_{stoc}	0.45	0.61
K_{cap}	1.23	1.52
$K_{ohm,sh}$	0.407	0.236
K_v	0.83	0.78

References. [1, Sec. 11.2; 2]

To explore the various approximations described above, and to achieve more realistic results, we have made a number of refinements to the model:

(1) The slot voltage in the Child law is the voltage across the sheath between the plasma and the surface of the confinement ring. If the confinement rings are quartz insulators, as in the experiments, then there is a voltage divider that relates the slot plasma-to-earth voltage to the slot plasma-to-quartz surface voltage. Approximating the sheath to be a vacuum dielectric, we find

$$\overline{V} = K_{\rm v}(\widetilde{V}_d + \widetilde{V}_b)\frac{s}{s + (l-g)/2\kappa_q} + 4.8\,{\rm T}_e \tag{7}$$

where κ_q is the dielectric constant of the quartz. We note that this reduces the voltage across the slot and consequently increases the pinch-off length $w_{\rm po}$ at a given voltage. Quantitatively, the change in length is of the order of 10 to 15 percent.

(2) A more general approach to the diffusion that is useful over a wider range of pressures equates the rate of change of the radial flux Γ_x to the local axial (along z) loss:

$$\frac{d}{dx}(\Gamma_x(x)d(x)) = -2\,n(x)h_l(x)u_B \tag{8}$$

with

$$h_l(x) = \frac{0.86}{(3 + d(x)/2\lambda_i)^{1/2}} \tag{9}$$

the edge-to-center density ratio given by low pressure diffusion theory [1, Eq. (5.3.13)], and with $d(x) = g - 2s(x)$ the bulk plasma thickness. For lower pressures, Γ_x depends in a nonlinear way on the density n [1, Sec. 5.3]

$$\Gamma_x = n(x)u_{ix}(x) \approx -\frac{2e{\rm T}_e}{\pi M}\frac{\lambda_i}{\langle u_i\rangle}\frac{dn}{dx} \tag{10}$$

where u_i is the (radial) diffusion velocity along the slot, and $\langle u_i\rangle \approx u_B/2$ is an average flow velocity over the axial cross section. We have evaluated this non-linear diffusion model in various approximations by integrating (8) and (10) along with the relations (3), (7), and (9), finding decay lengths larger than g/π by about 10 to 15 percent. The finite thickness of the sheath, and the variation of the sheath size with changing density are found to have minor effects on the decay length, because $d = g - 2s$ and $s \ll g$ over the high densities in most of the slot.

(3) At high pressures, the sheaths become collisional, such that the collisionless Child law is replaced with the collisional form (see Table 1). For $\lambda_i \ll g$, this results in a decreased pinch-off density, compared to the collisionless case, and therefore to a slightly increased pinch-off length, of 5 to 10 percent.

(4) Another physical quantity that leads to longer decay lengths is ionization within the slot. To calculate this effect, we examined the high pressure diffusion equation (1), except that we included the ionization

$$-D_a\nabla^2 n = \nu_{\rm iz} n \tag{11}$$

where ν_{iz} is the ionization frequency of the main discharge. This equation was solved as in (2) by separation of variables, giving, with the same approximation as in (2) that $n = 0$ at $z = \pm g/2$, the decay length

$$\Lambda = \frac{g/\pi}{(1 - \nu_{iz} g^2 / D_a \pi^2)^{1/2}} \tag{12}$$

This results in 5 to 10 percent longer decay length than that obtained from (2) in the absence of ionization.

We examined effects (1)-(3) quantitatively and compared the final results to the simple high pressure model. Figure 3 shows the decay of the slot density n versus position x for a main discharge with $l = 3$ cm and a slot width of $g = 0.5$ cm, with quartz filling the remaining width. The collisionless Child law was used, with discharge parameters: main discharge density $n_e = 2 \times 10^{11}$ cm^{-3} and dc sheath voltage $\overline{V} = 100$ V at 50 mTorr in argon. The solid line gives the density decay using the nonlinear diffusion model, including the effects of the voltage division between the sheath and quartz capacitances, and including the effects of the spatially-varying sheath thickness. Omitting the latter effect yields the dashed line. The dotted line gives the decay using the simple high pressure diffusion theory. The pinch-off density for these parameters is indicated by the dotted horizontal line. We see that the nonlinear diffusion model increases the pinch-off length by about 30 percent compared to the high pressure model, but cannot account for the transition to peripheral ignition, at about the above parameters, seen in some experiments. In Fig. 4 we show the results at a higher pressure, 200 mTorr, comparing the results of the collisionless and collisional sheath models.

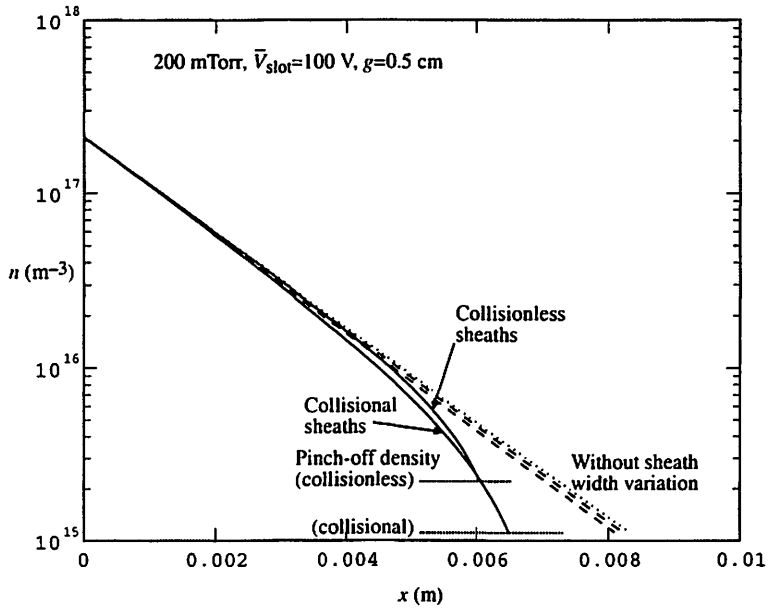

Figure 4. Plasma density in the slot versus position at 200 mTorr in argon, showing the the variation in pinch-off length w_{po} for collisionless and collisional sheath models.

The conclusions are that for a slot length w exceeding the pinch-off length, typically about 1 cm, diffusion of plasma from the main discharge into the slot is not sufficient to ignite a peripheral plasma. However, the diffusing plasma is highly conductive and carries the rf potential of the main discharge into the slot, thus increasing the capacitive coupling from the main discharge to the periphery. The increased coupling can lead to ignition of the peripheral plasma, provided that the maintenance condition for a peripheral discharge is met. We consider discharge maintenance conditions in the following two sections of the report.

III. CAPACITIVE DISCHARGE MAINTENANCE

The condition on rf voltage versus pressure for which a capacitive rf discharge can just be maintained is known as the maintenance curve. The main feature of maintenance is that the total width of the sheaths approaches closely the gap spacing, leading to a thin bulk plasma and a rise in electron temperature. The ionization balance in the bulk or the electron power balance of the discharge is then lost, and the discharge extinguishes. The sheath becomes large at either very low or very high rf voltages, yielding a double-valued maintenance curve. Some measurements of maintenance can be found in the literature for argon [3–6] and some molecular gases [7] at moderate pressures (below 1 Torr) over a limited range of discharge gap sizes. Measurements of electrical characteristics, but not extinction, over a wide range of pressures and voltages have been reported in argon [8].

Figure 5 illustrates the simple one-dimensional symmetric model that we use to determine the maintenance curves. The discharge gap width is L, and the dielectrics each have a thickness $L_q/2$ and relative dielectric constant κ_q.

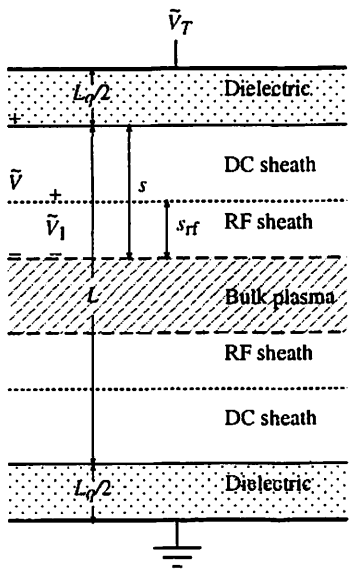

Figure 5. Symmetric one-dimensional capacitive discharge model.

At low rf voltages, new physics enters into the description of rf discharges, beyond that included in the standard global model [1, Sec. 11.2]:

(1) A dc sheath voltage and dc sheath width exist in the absence of an rf voltage across the sheath (see Fig. 5). These dc effects are neglected in simple global models. We include these effects by using (4) to relate the dc and rf voltages.

(2) Because the sheath includes both rf and dc parts, the rf voltage drop $\widetilde{V}$ across the entire sheath is not the same as the rf voltage drop $\widetilde{V}_1$ across the rf-part of the sheath (see Fig. 5). In the discussion below, we give the relation between these two voltages.

(3) In the standard model, the total voltage drop across the discharge gap L is approximated by the reactive voltage drop across the sheaths alone. To determine the maintenance condition, the reactive voltage drop across the bulk plasma and the resistive voltage drops due to the electron and ion power absorption must be included in the analysis.

(4) There is a transition from ambipolar to free diffusion of electrons in the bulk plasma (width $d = l - 2s$) when d becomes of order of four Debye lengths [9]. The transition increases the electron loss rate by a factor of $T_e/2T_i$, which is typically 20–100. This large increase in loss rate extinguishes the discharge. We have accounted for this effect by requiring that the bulk plasma be at least four Debye lengths thick.

Including these considerations, in the steady state, the production of electron-ion pairs in the volume by electron-neutral ionization is balanced by the loss of pairs to the walls:

$$K_{iz} n_g n d = 2\, h_l n u_B \tag{13}$$

Here $K_{iz}(T_e)$ is the ionization rate coefficient (See Table 2), n_g is the neutral gas density, n is the central plasma density, $d = L - 2s$ is the quasineutral bulk plasma thickness, with s the maximum (rf+dc) sheath thickness, and h_l is the edge-to-center density ratio given by (9). It is well known that this particle (ion) balance relation sets the electron temperature T_e of the plasma, independent of the plasma density n_e. Typically $T_e \sim 2$–5 eV, depending weakly on the pressure.

Table 2. Rate Coefficients and Threshold Energies for Argon

Rate Coefficient (m^3/s)	Threshold Energy (V)
$K_{el} = 2.336 \times 10^{-14}\, T_e^{1.609}\, \exp\left(0.0618(\ln T_e)^2 - 0.1171(\ln T_e)^3\right)$	
$K_{iz} = 2.34 \times 10^{-14}\, T_e^{0.59} \exp(-17.44/T_e)$	$\mathcal{E}_{iz} = 15.76$
$K_{ex} = 2.48 \times 10^{-14}\, T_e^{0.33} \exp(-12.78/T_e)$	$\mathcal{E}_{ex} = 12.14$

Note. T_e is in the range 1–7 eV; *reference* [1, Second Edition, Chapter 3]

The corresponding electron power balance relation is

$$S_e = 2\,eh_l n u_B(\mathcal{E}_c + \mathcal{E}'_e) \tag{14}$$

where S_e is the power per unit area absorbed by electrons from the rf field,

$$\mathcal{E}_c(\mathrm{T_e}) = \mathcal{E}_{iz} + \mathcal{E}_{ex}K_{ex}/K_{iz} + 3(m/M)\mathrm{T_e}K_{el}/K_{iz} \tag{15}$$

is the sum of the collisional electron energy losses from ionization, excitation, and elastic scattering per electron-ion pair created (typically $\mathcal{E}_c \sim 30$–100 eV for argon, depending on the pressure), and $\mathcal{E}'_e(\mathrm{T_e})$ is the electron kinetic energy lost from the plasma per electron-ion pair created ($\mathcal{E}'_e \approx 6.8\,\mathrm{T_e}$ for argon). We see that the density is proportional to the electron power absorbed. There are three mechanisms for electron power absorption from the rf source:

(1) Stochastic heating yields a time-average electron power absorption for each sheath

$$S_{stoc} = K_{stoc}\left(\frac{m}{e}\right)^{1/2}\epsilon_0\omega^2\mathrm{T_e}^{1/2}\widetilde{V}_1 \tag{16}$$

(2) Ohmic heating in the bulk plasma yields

$$S_{ohm} = K_{ohm}\frac{m}{2e}h_l\epsilon_0\omega^2\nu_m d\,\mathrm{T_e}^{1/2}\widetilde{V}_1^{1/2} \tag{17}$$

(3) Ohmic heating in each sheath yields

$$S_{ohm,sh} = K_{ohm,sh}\frac{m}{2e}\epsilon_0\omega^2\nu_m s\widetilde{V}_1 \tag{18}$$

Here V_1 is the rf voltage across the rf-part of the sheath, and ν_m is the electron-neutral momentum transfer frequency. Summing these powers gives

$$S_e = 2S_{stoc} + 2S_{ohm,sh} + S_{ohm} \tag{19}$$

Since $S_e \propto \omega^2$, the low frequency bias source contributes negligibly to the electron power absorption, and therefore, to the plasma density. The total power per unit area S_{abs}, absorbed from the high frequency source, includes both S_e and the ion power per unit area

$$S_i = 2\,eh_l n_e u_B \mathcal{E}_i \tag{20}$$

where $\mathcal{E}_i = \overline{V}$ is the dc voltage across each sheath, given by (4).

The rf current density flowing through the sheath can be written as

$$\tilde{J} = K_{cap}\frac{j\omega\epsilon_0}{s_{rf}}\widetilde{V}_1 = K_{cap}\frac{j\omega\epsilon_0}{s}\widetilde{V} \tag{21}$$

The relation between $\widetilde{V}_1$ and $\widetilde{V}$ can be found by noting that the electron powers (16)–(18) are functions of $|\tilde{J}|^2/n_s$, with $|\tilde{J}|^2/n_s \propto \widetilde{V}_1^{1/2}$ in the standard model [1, p. 344]. For example, the ohmic heating power in the bulk plasma is $S_{\rm ohm} = \frac{1}{2}|\tilde{J}|^2/\sigma_{\rm dc} d$, with $\sigma_{\rm dc} = e^2 n/m\nu_m$, yielding $S_{\rm ohm} \propto h_l \nu_m d|\tilde{J}|^2/n_s$. Eliminating s from the RHS of (21) by using the Child law (3), we obtain

$$\frac{|\tilde{J}|^2}{n_s} = K_{\rm cap}^2 \omega^2 \epsilon_0 e \left(\frac{M}{2e}\right)^{1/2} \frac{u_B}{K_{\rm CL} K_{\rm v}^{3/2}} \frac{\widetilde{V}^2}{(\widetilde{V} + 4.8\,{\rm T}_e/K_{\rm v})^{3/2}} \tag{22}$$

In the limit that $K_{\rm v}\widetilde{V} \gg 4.8\,{\rm T}_e$, the last (voltage-dependent) term in (22) reduces to the standard model result $\widetilde{V}_1^{1/2}$. Therefore (22) generalizes the standard model result for $|\tilde{J}|^2/n_s$, from which we see that the rf voltage $\widetilde{V}_1$ across the rf-part of the sheath is related to the total rf voltage $\widetilde{V}$ across the sheath by

$$\widetilde{V}_1 = \frac{\widetilde{V}^4}{(\widetilde{V} + 4.8\,{\rm T}_e/K_{\rm v})^3} \tag{23}$$

From the last two terms in (21), we also obtain the rf sheath thickness

$$s_{\rm rf} = s\left(\frac{\widetilde{V}}{\widetilde{V} + 4.8\,{\rm T}_e/K_{\rm v}}\right)^3 \tag{24}$$

The effective resistance seen by the driving voltage source, accounting for stochastic heating, ohmic heating in the sheath, and ion energy losses, is given by

$$R_{\rm eff} = 2\frac{S_{\rm stoc} + S_{\rm ohm,sh} + S_i}{|\tilde{J}|^2} \tag{25}$$

We will account separately for the resistance of the bulk plasma using a complex κ_p, as given in (27) and (28), below. The total rf voltage V_T across the discharge is the sum of the voltages across the plasma and the dielectric (see Fig. 5)

$$\widetilde{V}_T = \widetilde{V}_{\rm pl} + \widetilde{V}_{\rm diel} \tag{26}$$

where

$$\widetilde{V}_{\rm pl} = \frac{1}{j\omega\epsilon_0}\left(\frac{2s}{K_{\rm cap}} + \frac{d}{\kappa_p}\right)\tilde{J} + R_{\rm eff}\tilde{J} \tag{27}$$

and

$$\widetilde{V}_{\rm diel} = \frac{1}{j\omega\epsilon_0}\frac{L_q}{\kappa_q}\tilde{J} \tag{28}$$

with

$$\kappa_p = 1 - \frac{\omega_p^2}{\omega(\omega - j\nu_m)} \tag{29}$$

the bulk plasma dielectric constant, $\omega_p = (e^2 n/\epsilon_0 m)^{1/2}$ the plasma frequency and ν_m the electron-neutral collision frequency.

The model equations are numerically solved as follows: First we choose a vector of values for the sheath thickness s. Next, using $d = L - 2s$, we solve the particle balance (13) to determine ${\rm T}_e$. Then we substitute

S_e from (19) into the LHS of the electron power balance (14) and use the Child law (3) to eliminate the density in the RHS of (14). The resulting equation is a ninth-order polynomial equation for the variable $\sqrt{\widetilde{V}}$. We find that for a given value of s, there are two (or zero) valid roots, which are the maximum and minimum real positive roots with $\sqrt{\widetilde{V}} > \sqrt{(\widetilde{V}_b + 4.8\,\mathrm{T}_e)/K_\mathrm{v}}$. Having determined $\widetilde{V}$, all other quantities, such as the powers, discharge current density $\widetilde{J}$, and total voltage $\widetilde{V}_T$, are evaluated. To find the maintenance voltage at a given pressure, we then determine the minimum (and maximum) rf voltage $\widetilde{V}_T$ for which a solution exists and for which the bulk plasma width exceeds a certain fixed number of Debye lengths. In this report we have chosen (somewhat arbitrarily) $d > 4\,\lambda_{Ds}$. In practice, this constraint on the bulk plasma thickness does not affect the maintenance condition for most of the parameters of interest.

Figure 6 shows recent measurements of maintenance [3] (squares), along with the model results, for a symmetric capacitive discharge with $L = 2.2$ cm driven at 13.56 MHz. (There is no dielectric.) The model shows the same form as the measurements for the lower branch of the maintenance curve, but with the minimum pressure for maintenance shifted from about 20 mTorr in the experiment to about 12 mTorr in the model. The upper branch is seen in the model, but not in the measurements which were limited to $V_\mathrm{rf} < 500$ V. However, double-valued maintenance curves have been measured experimentally for molecular gases [7].

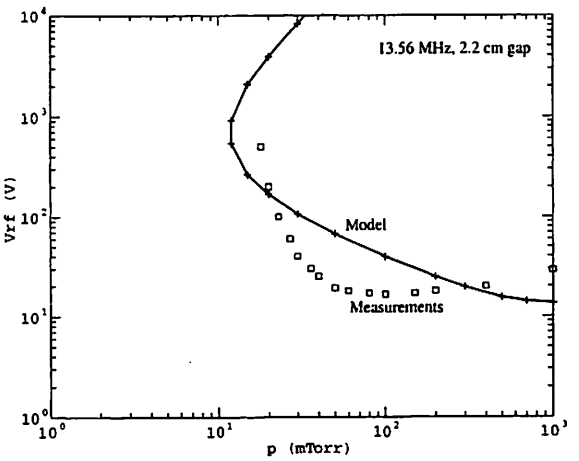

Figure 6. Measured and calculated maintenance voltage versus pressure for a 2.2 cm gap driven at 13.56 MHz in argon.

The α-to-γ transition may play a role in discharge maintenance. This transition is due to a "Paschen-like" breakdown of the sheath due to secondary emission from the discharge plates ($\gamma_\mathrm{se} > 0$). When the Paschen voltage exceeds the dc voltage across the sheath, then the sheath "breaks down", and the discharge enters the γ-mode. While Paschen breakdown is not a concern at low pressures, it can be a significant issue at pressures exceeding a few hundred mTorr in argon. As a result, we implemented a calculation of Paschen breakdown in the sheath in the maintenance model. Using an effective secondary emission coefficient of

$\gamma_{se} = 0.3$, we find an α-γ transition in the model, which, however, does not influence the lower branch of the extinction curve, in agreement with the measurements at pressures above 100 mTorr. However, the measurements show some residual secondary emission effects at lower pressures, which are not captured in the model. The multipactor effect [10–12] may also play a role in maintenance at the lower pressures.

IV. TWO-DIMENSIONAL EFFECTS ON DISCHARGE MAINTENANCE

Because the slot is driven at one end (its inner radius) by the rf voltage of the main discharge plasma, with its top and bottom surfaces earthed through the quartz confinement rings, a large radial component of the rf current flows along the slot when a slot plasma is ignited. The radial current further increases when a peripheral plasma is also ignited, which draws its current through the slot. Furthermore, the two sheaths near the top and bottom earthed conductors see the same voltage, and therefore oscillate in-phase with each other, rather than 180° out-of-phase, as for the conventional discharge shown in Fig. 5.

To account for the in-phase motion, we can solve the conventional out-of-phase discharge model, with modifications to the ohmic power deposition discussed below, to determine the total voltage $\tilde{V}_T$. By symmetry, the main discharge voltage for the in-phase situation is then $\tilde{V}_d = \tilde{V}_T/2$.

To determine the modification of the ohmic power for the in-phase situation, we examine the time-varying ohmic power dissipated in the slot

$$P_{\text{ohm}}(t) = \int_0^w dx \int_{-d(t)/2}^{d(t)/2} dz \frac{|\tilde{\mathbf{J}}(x,z,t)|^2}{\sigma_{\text{dc}}} \tag{30}$$

where

$$\tilde{\mathbf{J}} = \hat{x}\tilde{J}_x(x,z,t) + \hat{z}\tilde{J}_z(x,z,t) \tag{31}$$

is the rf current flowing in the slot plasma, $d(t)$ is the time-varying bulk width of the plasma, and the conductivity σ_{dc} is assumed to be a constant. For a conventional discharge with out-of-phase sheaths, the radial current $\tilde{J}_x \equiv 0$ and the axial current $\tilde{J}_z = \tilde{J}_0(t)$, independent of x and z. We assume a sinusoidal time variation for the current, $\tilde{J}_0 = J_0 \sin\omega t$, and we use a simple homogeneous density sheath model (neglecting the dc sheath component of the sheath thickness) to approximate the time-varying sheath motion. For the out-of-phase sheath oscillations, the two sheath thicknesses are

$$s_{1,2}(t) \approx \frac{s}{2}(1 \pm \cos\omega t) \tag{32}$$

We see from (32) that $s_1 + s_2 = s$ and $d(t) = L - s \equiv d_{\text{ave}} = \text{const}$. Using these expressions to integrate (30), and averaging over an rf period, we obtain

$$P_{\text{ohm}} = \frac{1}{2} w d_{\text{ave}} \frac{J_0^2}{\sigma_{\text{dc}}} \tag{33}$$

For in-phase excitation, we assume that $\widetilde{\mathbf{J}} \propto \widetilde{\mathbf{E}}$, with the electric field $\widetilde{\mathbf{E}}$ a solution determined by solving Laplace's equation for the potential in the slot. Assuming open circuit boundary conditions $\tilde{J}_x = 0$ at $x = 0$, corresponding to no flow of current from the slot into the periphery, then the solution is

$$\tilde{J}_x = -2\tilde{J}_0(t)\frac{x}{d(t)}, \qquad \tilde{J}_z = 2\tilde{J}_0(t)\frac{z}{d(t)} \tag{34}$$

Inserting these expressions into (30) and integrating yields

$$P_{\rm ohm}(t) = \left[\frac{wd(t)}{3} + \frac{4w^3}{3d(t)}\right]\frac{\tilde{J}_0^2(t)}{\sigma_{\rm dc}} \tag{35}$$

For a sinusoidal time variation of the current, we obtain from (32) (with $\pm \rightarrow +$ for both sheaths) that $d(t) = d_{\rm ave} - s\cos\omega t$ for in-phase sheath motion, where, again, $d_{\rm ave} = L - s$. Performing the time-averages using this $d(t)$ then yields

$$P_{\rm ohm} = \frac{1}{2}\frac{\bar{J}_0^2}{\sigma_{\rm dc}} w d_{\rm ave}\eta \tag{36}$$

where

$$\eta = \frac{1}{3} + \frac{8w^2}{3s^2}\left(1 - \sqrt{1 - \frac{s^2}{d_{\rm ave}^2}}\right) \equiv \eta_{\rm oc} \tag{37}$$

Comparing (36) together with (37) to (33), $\eta_{\rm oc}$ is the *ohmic enhancement factor* due to the geometry of the in-phase sheath motion, when the periphery draws no current. The second term in $\eta_{\rm oc}$ varies from $32w^2/3L^2$ as $s \rightarrow L/2$ (and $d_{\rm ave} \rightarrow L/2$) to $4w^2/3L^2$ as $s \rightarrow 0$ (and $d_{\rm ave} \rightarrow L$). The ohmic powers (17) and (18) in the model of Sec. III are multiplied by $\eta_{\rm oc}$ to determine the maintenance curve for the slot when there is no peripheral plasma.

When a peripheral plasma exists, then an additional current $\tilde{I}_{\rm per}$ is drawn through the slot, leading to an additional ohmic power dissipation. We assume that $\tilde{I}_{\rm per} = j\omega C_{\rm per}\tilde{V}_d$, with $C_{\rm per} = K_{\rm cap}\epsilon_0 l_{\rm eff}/s_{\rm eff}$, with $l_{\rm eff}$ and $s_{\rm eff}$ the effective width and sheath thickness of the peripheral plasma, chosen heuristically from the peripheral geometry. For example, for a periphery with $w_{\rm per} \ll l$ (see Fig. 1), we choose $l_{\rm eff} = l$ and $s_{\rm eff}$ to be a typical sheath width in an ignited peripheral plasma. The capacitance $C_{\rm per}$ is in parallel with the series combination $C_{\rm sl} = 2K_{\rm cap}\epsilon_0 w\kappa_q/(2\kappa_q s + K_{\rm cap}l_q)$ of the sheath and quartz capacitances in the slot, with $l_q = l - g$ the total quartz thickness. Then the ratio of the peripheral and slot currents is

$$\frac{\tilde{I}_{\rm per}}{\tilde{I}_0} = \frac{C_{\rm per}}{C_{\rm sl}} = \frac{l_{\rm eff}(2s\kappa_q + K_{\rm cap}l_q)}{2w\kappa_q s_{\rm eff}} \tag{38}$$

Using $\tilde{I}_{\rm per} = \tilde{J}_{x\rm per}\, d(t)$ and $\tilde{I}_0 = \tilde{J}_0 w$, we obtain in place of the $\tilde{J}_x$ current in (34)

$$\tilde{J}_x = -\frac{\tilde{J}_0}{d(t)}\left(2x + \frac{C_{\rm per}}{C_{\rm sl}}w\right) \tag{39}$$

Using (39) in (30) and integrating to evaluate the ohmic power, and performing the time averages, we obtain (36) with

$$\eta = \eta_{\rm oc} + 4\frac{w^2}{s^2}\frac{C_{\rm per}}{C_{\rm sl}}\left(1 + \frac{1}{2}\frac{C_{\rm per}}{C_{\rm sl}}\right)\left(1 - \sqrt{1 - \frac{s^2}{d_{\rm ave}^2}}\right) \equiv \eta_{\rm per} \tag{40}$$

The last term in (40) gives the enhancement in ohmic heating due to the current flow into the periphery. The ohmic powers (17) and (18) in the model of Sec. III are multiplied by $\eta_{\rm per}$ in (40) to determine the maintenance curve for the slot when a peripheral plasma is ignited.

We consider now the maintenance condition for plasma in the periphery when there is no plasma in the slot. Then the main discharge voltage $\widetilde{V}_d$ couples capacitively across the dielectric confinement rings to the periphery, igniting a conventional capacitive discharge in the periphery having two out-of-phase sheaths. Since the slot is thin, $g \ll l$, we assume that the entire gap l is filled with dielectric. We let the peripheral plasma voltage and current at the slot exit (taken as $x = 0$) be $\widetilde{V}_{\rm pl}$ and $\tilde{I}_{\rm pl}$, where $\widetilde{V}_{\rm pl}$ is given by (27) and where $\tilde{I}_{\rm pl} = \tilde{J}l$, with $\tilde{J}$ given by (21). For given values of $\widetilde{V}_{\rm pl}$ and $\tilde{I}_{\rm pl}$, the voltage $\widetilde{V}_d$ at the slot entrance $x = w$ is determined from a two-dimensional solution of Laplace's equation within the dielectric. Considering the fundamental Fourier mode, the potential in the dielectric is

$$\Phi(x,z) = \cos\frac{\pi z}{l}\left(A_1\cosh\frac{\pi x}{l} + A_2\sinh\frac{\pi x}{l}\right) \tag{41}$$

At the slot exit, $\Phi(0,0) = A_1 = 4\widetilde{V}_{\rm pl}/\pi$. The factor of $4/\pi$ gives the fundamental mode amplitude for a voltage $\widetilde{V}_{\rm pl}$ in the peripheral plasma that is uniform along z. Using $\mathbf{E} = -\nabla\Phi$, the x-component of the electric field at $x = 0$ is

$$E_x = -A_2\frac{\pi}{l}\cos\frac{\pi z}{l} \tag{42}$$

The displacement current flowing in the dielectric at the slot exit is

$$I_{\rm pl} = \int_{l/2}^{l/2} j\omega\epsilon_0\kappa_q A_2\frac{\pi}{l}\cos\frac{\pi z}{l}\,dz \tag{43}$$

which yields $A_2 = I_{\rm pl}/(2j\omega\epsilon_0\kappa_q)$. The voltage in the main discharge at the slot entrance is $\widetilde{V}_d = \pi\Phi(w,0)/4$. Substituting A_1 and A_2 determined above into (41) to evaluate $\Phi(w,0)$, we find

$$\widetilde{V}_d = \widetilde{V}_{\rm pl}\cosh\frac{\pi w}{l} + \frac{\pi}{4}\frac{l}{2j\omega\epsilon_0\kappa_q}\tilde{J}\sinh\frac{\pi w}{l} \tag{44}$$

Equation (44) replaces (26) in determining the main discharge rf voltage when the peripheral plasma is ignited and there is no plasma in the slot.

If there is diffusion of plasma into the slot, but the slot is not ignited, then (44) is slightly modified. We assume a triangular axial voltage variation at the position of plasma pinch-off $w_{\rm po}$ within the slot. Then we find for the fundamental mode that $\widetilde{V}_d = \pi^2\Phi(w - w_{\rm po},0)/8$, replacing $\widetilde{V}_d = \pi\Phi(w,0)/4$ in the preceding analysis, yielding

$$\widetilde{V}_d = \frac{32}{\pi^3}\widetilde{V}_{\rm pl}\cosh\left(\pi\frac{w - w_{\rm po}}{l}\right) + \frac{8}{\pi^2}\frac{l}{2j\omega\epsilon_0\kappa_q}\tilde{J}\sinh\left(\pi\frac{w - w_{\rm po}}{l}\right) \tag{45}$$

Equation (45) replaces (26) in determining the main discharge rf voltage when the peripheral plasma is ignited and there is a diffusion "finger" of plasma in the slot.

When both slot and periphery are ignited, then the peripheral region is directly connected to the main discharge by the ignited slot plasma. The rf voltage driving the peripheral plasma is then the main discharge voltage $\widetilde{V}_d$, and the two sheaths at the upper and lower earthed surfaces of the periphery move in phase with each other. Therefore, we use an in-phase model with no capacitive voltage drops across dielectric surfaces to determine the maintenance condition of the periphery when the slot is ignited.

For the preceding analysis in this section, we have assumed that the rf voltage is radially uniform within a diffusion or ignited slot plasma. To justify this assumption, it is necessary to consider the wave propagation effects within a slot containing a plasma. We use a simple quasistatic analysis to determine the propagation characteristics. As shown in Fig. 7, we consider a uniform density plasma slab of thickness $2l_p$ lying between two dielectric slabs, each having thickness l_q.

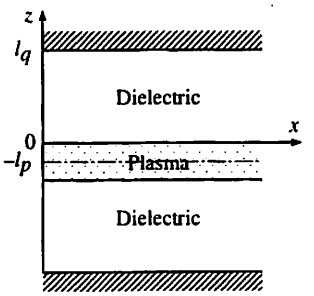

Figure 7. Model for surface wave propagation in plasma-filled slot.

Choosing the x-axis to lie along the plasma-dielectric interface, with the plasma located at $0 > z > -l_p$ and the top dielectric at $0 < z < l_q$, then the potentials for a single, symmetrically-excited quasistatic wave propagating along x are

$$\Phi_p = A_p \, \mathrm{e}^{-jkx} \cosh k(l_p + z), \qquad \Phi_q = A_q \, \mathrm{e}^{-jkx} \sinh k(l_q - z) \tag{46}$$

where k is the (complex) propagation constant for the wave. The wave amplitude has its maximum value at the plasma-dielectric interface $z = 0$, decaying both into the plasma and into the dielectric, and is therefore known as a *surface wave*. The z-components of the electric fields are

$$E_{zp} = kA_p \, \mathrm{e}^{-jkx} \sinh k(l_p + z), \qquad E_{zq} = kA_q \, \mathrm{e}^{-jkx} \cosh k(l_q - z) \tag{47}$$

Using the boundary conditions at $z = 0$ that $\Phi_p = \Phi_q$ and that $\kappa_p E_{zp} = \kappa_q E_{zq}$, where κ_p and κ_q are the relative dielectric constants of the plasma and insulator, we obtain the dispersion relation for the waves

$$-\kappa_p \tanh kl_p = \kappa_q \coth kl_q \tag{48}$$

Assuming that the characteristic wavelength $2\pi/|k|$ is long compared to plasma and dielectric thicknesses, we can expand the cosh and sinh functions to obtain

$$k^2 = -\frac{\kappa_p}{\kappa_q} \frac{1}{l_q l_p} \tag{49}$$

At high pressures, the plasma is collisional ($\nu_m \gg \omega$), and from (29) we approximate $\kappa_p \approx -j\omega_p^2/\omega\nu_m$. Inserting this into (49), we obtain

$$k = \frac{1+j}{\sqrt{2}} \left(\frac{\kappa_q}{l_p l_q} \frac{\omega \nu_m}{\omega_p^2} \right)^{1/2} \tag{50}$$

Now consider a situation in which a plasma is maintained in the slot with the peripheral plasma not ignited. This corresponds to an open-circuited boundary condition at the slot exit $x = 0$. The incident wave then excites a reflected wave at the slot exit. The sum of incident and reflected waves yields a standing wave along x, for which the exponential factor e^{-jkx} in (46) is replaced by the factor $\cos kx$, corresponding to a zero-derivative of the voltage with respect to x at the open circuit. Then the ratio of the exit-to-entrance voltage is $|\sec kw|$, with k still given by (50).

As an example, we estimate the voltage ratio for maintenance of a slot plasma of length $w = 3$ cm under open-circuited conditions at 200 mTorr. The maintenance density is $n \approx 10^9$ cm^{-3}, the collision frequency is $\nu_m \approx 3.3 \times 10^8$ s^{-1}, and the radian frequency is 1.76×10^8 s^{-1}, yielding $\omega_p^2/\omega\nu_m \approx 55.1$. We assume a slot thickness of 0.5 cm that is half-filled with plasma, corresponding to $l_p = 0.125$ cm, and we take $l_q = l/2 = 1.5$ cm. Then (50) yields $k \approx 0.44(1+j)$ cm^{-1}, and the voltage ratio is $|\sec kw| \approx 0.57$. At 100 mTorr, n is about a factor of two higher, and ν_m is a factor of two lower, yielding $k \approx 0.22(1+j)$ cm^{-1}, and $|\sec kw| \approx 0.94$. Hence for this example the voltage is reasonably uniform in the slot for pressures less than about 200 mTorr.

The preceding results are for a quasistatic analysis. We have compared this analysis to a more complete analysis based on the full set of electromagnetic equations for this surface wave [13]. The quasistatic analysis agrees well with the electromagnetic analysis for the range of parameters of interest.

Incorporating the two-dimensional effects of this section into the model of Sec. 3, we calculate the maintenance curves for the nominal set of parameters: high frequency $f = 27.1$ MHz, low frequency bias voltage $\widetilde{V}_b = 0$, gap thickness $l = 3$ cm, slot thickness $g = 0.5$ cm, slot width $w = 3$ cm, periphery width $w_{\text{per}} = 3$ cm, and quartz dielectric constant $\kappa_q = 2$, with collisional sheaths. In Fig. 8, we show five curves for the following five conditions:

(a) Slot maintenance with no ignited peripheral plasma. We use in-phase sheaths with η_{oc} given in (37), $L = g$ and $L_q = l - g$ (see Fig. 5 and Fig. 1), and $\widetilde{V}_T$ given in (26), with $\widetilde{V}_d = \widetilde{V}_T/2$.

(b) Slot maintenance with an ignited peripheral plasma. We use in-phase sheaths with η_{per} given in (40), $L = g$, $L_q = l - g$, $w_{\text{eff}} = l$, $s_{\text{eff}} = 0.4l/\sqrt{2}$, and $\widetilde{V}_T$ given in (26), with $\widetilde{V}_d = \widetilde{V}_T/2$.

(c) Periphery maintenance with no plasma in the slot. We use out-of-phase sheaths with $L = l/\sqrt{2}$ and $L_q = 0$, with $\widetilde{V}_d$ given in (44).

(d) Periphery maintenance with a 1 cm diffusion plasma in the slot. We use out-of-phase sheaths with $L = l/\sqrt{2}$, $L_q = 0$, and $w_{\text{po}} = 1$ cm, with $\widetilde{V}_d$ given in (45).

(e) Periphery maintenance with an ignited plasma in the slot. We use in-phase sheaths with η_{oc} given in (37), $L = l$, $L_q = 0$, $w = w_{\text{per}}$, and $\widetilde{V}_T$ given in (26), with $\widetilde{V}_d = \widetilde{V}_T/2$.

For example, at 100 mTorr, we see that the slot plasma will ignite at about 120 volts (curve a) and the periphery will ignite at about 190 volts (curve d). Hence, confinement is first lost by ignition of the slot plasma at this pressure, since once the slot ignites the periphery also ignites (curve e). However, for lower pressures, below about 40 mTorr, confinement is first lost by ignition of the periphery (curve d), which then causes the slot to also ignite (curve b). For pressures below 10 mTorr, the periphery ignites without igniting the slot.

In Fig. 9, we show the same five curves for a reduced slot thickness $g = 0.25$ cm and a correspondingly reduced pinch-off width, scaled from (6), of $w_{po} = 0.5$ cm. The thinner slot is much harder to ignite, and we see that confinement is lost due to ignition of the periphery (curve d) for pressures below about 190 mTorr. Figures 8 and 9 can be used to determine loss of confinement for different periphery and slot pressures. For example, for the nominal conditions of Fig. 8 with a 5 mTorr periphery pressure, confinement is lost by ignition of the slot plasma for slot pressures above 22 mTorr (curve a), and by ignition of the periphery plasma for slot pressures below 22 mTorr (curve d).

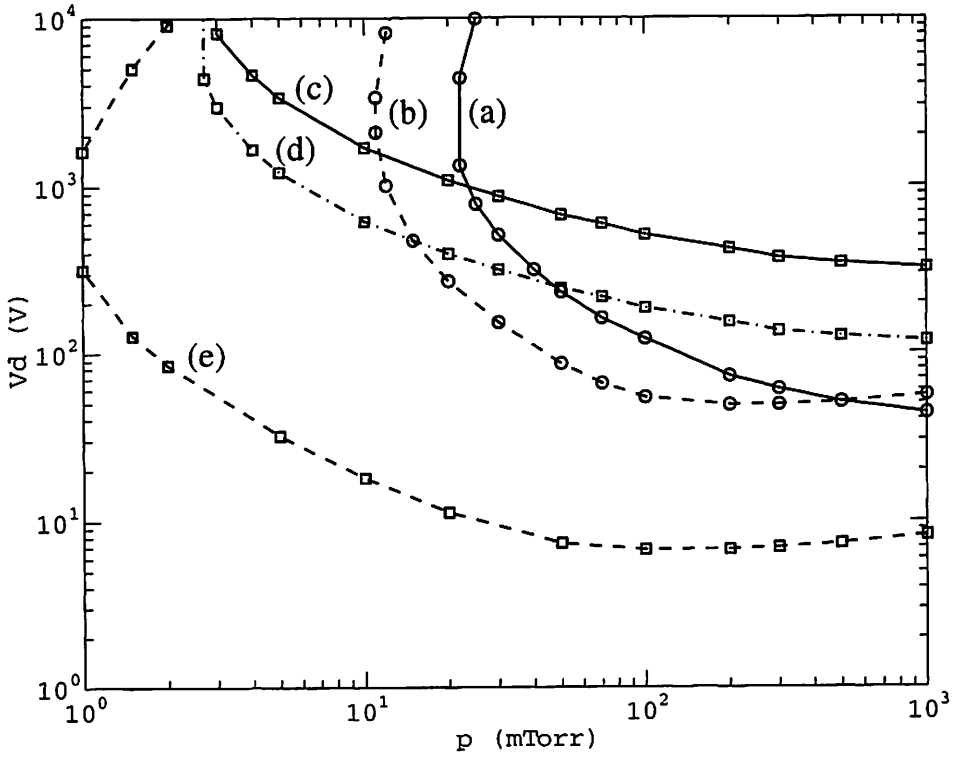

Figure 8. Maintenance curves for nominal conditions.

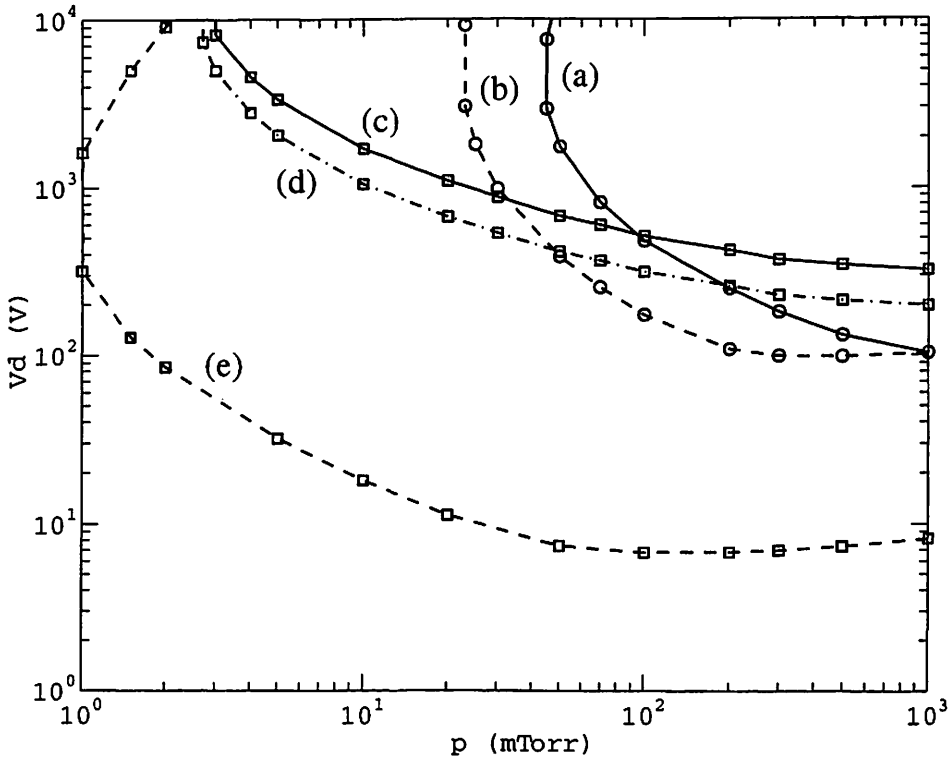

Figure 9. Maintenance curves for an 0.25 cm slot thickness and an 0.5 cm pinch-off width.

V. EXPERIMENTAL RESULTS

To examine the physics of plasma formation in slots and tubes connected to capacitive plasmas, we have designed and constructed a small confined dual frequency capacitive discharge (DFCD). Our DFCD chamber uses two 1.5 inch width (7 inch inner diameter, 10 inch outer diameter) quartz confinement rings. The gap width g can be varied as 1/4, 1/8, 1/16, and 1/32 inch, such that the effect of varying gap width on the plasma transport in the slot, and slot and edge plasma breakdown and maintenance, can be measured and compared with the models. The general specifications of the experiment are as follows: stainless steel chamber body and electrode, powered electrode diameter 5 inches, grounded electrode diameter 16 inches, electrode gap 1 inch, 2-way side pumping through 2 inch KF ports, Leybold Turbotronik NT 340M turbomolecular pump (340 liter/sec) with W.M. Welch rotary pump, ENI A500 power amplifier (500 W maximum power output at 0.3–35 MHz), dual (or triple) frequency wave generator, Advanced Energy Z-Scan RF measurement system, and an L-type matching network consisting of two vacuum Jennings capacitors (12–500 pF and 12–1000 pF each), a fixed capacitor (1600pF) and a 5 μH inductor.

To observe and measure the spatially varying optical emission from discharges, our chamber design provides two kinds of view ports. One is a 6 mm (1/4 inch) wide optical slot incorporated on the ground electrode with a quartz cover plate. Through this slot, we can observe the radial variation of optical emission from the main discharge, the quartz confinement rings, and the peripheral discharge, along the entire diameter

of the ground electrode. The other view ports are located at both ends of the two side extensions for the vacuum pump connection. These two quartz-covered view ports provide a side angle view into the peripheral region and the slot between the confinement rings. The time-varying floating potential near the slot entrance can be measured using a floating metal ring mounted near the inner diameter of one quartz confinement ring. This measurement will yield the various high and low frequency asymmetry factors, relating the driving voltages ($\widetilde{V}_{\rm rf}$, $\widetilde{V}_B$) to the main discharge voltages ($\widetilde{V}_d$, $\widetilde{V}_b$), to be incorporated into the models of diffusion and maintenance. There are two ports for capacitance manometers on the chamber, one in the main discharge region and one in the periphery. There are also two ports for mounting Langmuir probes, to measure electron temperatures and plasma densities in the main discharge and the peripheral discharge. A side view of the experiment in operation is given in Fig. 10.

Preliminary measurements with a single 27.12 MHz power source, using the widest gap width, indicate that a transition occurs with increasing power from a centrally confined plasma to a plasma that exists also in the slot and peripheral regions. Furthermore, as shown in Fig. 11, we have observed that a hysteresis occurs such that the maintenance of the peripheral plasma occurs at a lower power, when decreasing the power, than that required to create the peripheral discharge. These behaviors are qualitatively to be expected from our analysis. An unexpected phenomena was the observation, shown in Figs. 12 and 13, of both high frequency (kHz range) and low frequency (Hz range) relaxation oscillations, when plasma exists in the entire system (main, slot, and peripheral discharge). The existence of such oscillations prevents good matching. The phenomena is very interesting and merits detailed investigation.

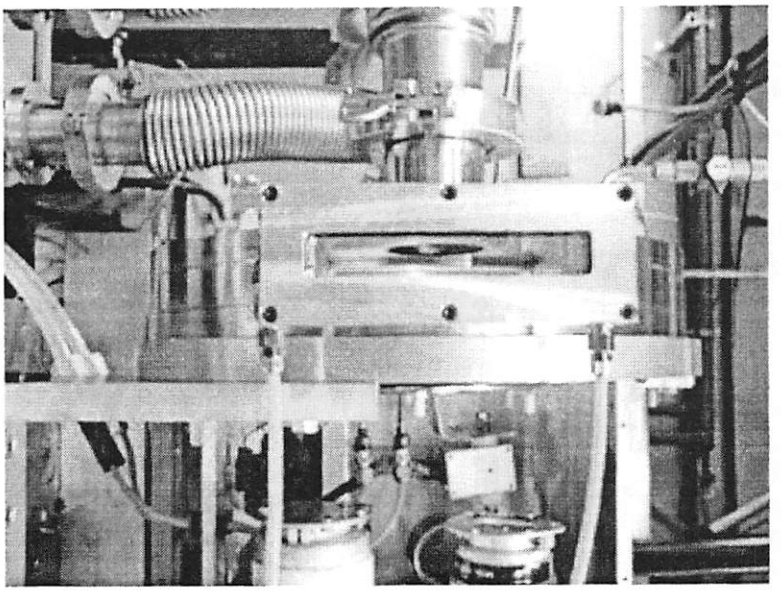

Figure 10. Side view of experiment, showing confined plasma between discharge plates.

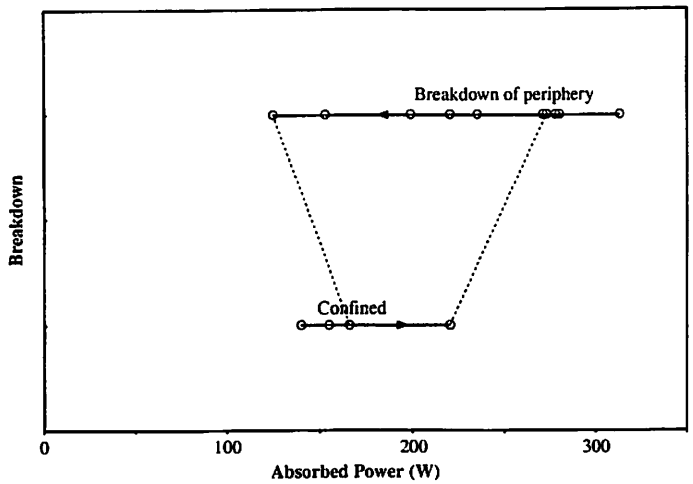

Figure 11. Hysteresis curve at 50 mTorr, with upper level indicating breakdown of peripheral plasma, and lower level indicating a confined plasma.

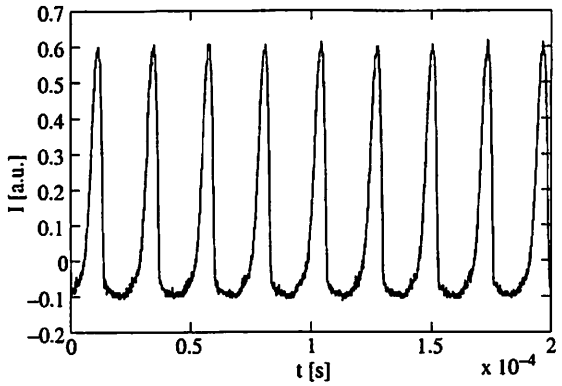

Figure 12. Time-varying optical emission I from the main discharge region, showing a high frequency (43.3 kHz) relaxation oscillation; 100 mTorr and 80 W absorbed power; the zero of I is not calibrated.

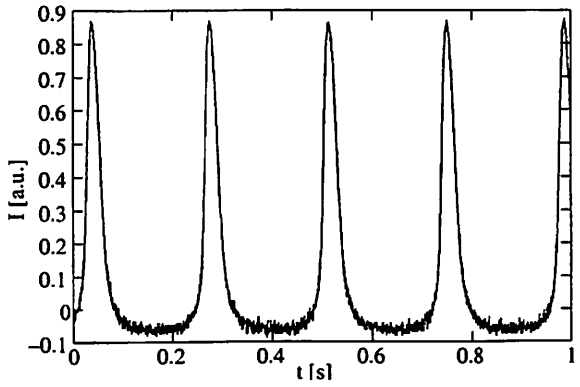

Figure 13. Time-varying optical emission I from the main discharge region, showing a low frequency (4.21 Hz) relaxation oscillation; 77 mTorr and 202 W absorbed power; the zero of I is not calibrated.

In the future, measurements of peripheral plasma ignition, maintenance, hysteresis, and relaxation oscillations will be made. Experiments, which are now in their preliminary stages, will cover all phases of the project. Verification of the predictions from the theoretical work described in the previous sections will be a main experimental objective. These include determination of the plasma diffusion, breakdown and maintenance scaling with pressure and power, with slot thickness as a parameter. The effect of hysteresis on these scalings will also be investigated. In addition, an important aspect of the experimental work will be measurements of the relaxation oscillations, with accompanying theoretical work to understand their behavior and scaling. Our previous considerable experience in observing and developing models of relaxation oscillations in electronegative plasmas[7-11] should be very helpful in this study. The mechanisms are, of course, different, with the required separation of the two time scales dependent on the geometry, rather than on electronegativity.

Some specific measurements to be done are the following. Spatially-varying optical emission from the main discharge, quartz confinement rings, and peripheral discharge will be measured along a diameter of the grounded electrode through the 6 mm wide optical viewport. The diagnostic will yield quantitative visual evidence of the transport and maintenance of plasma in the slot, which will be compared to the analytical models. The time-varying floating potential near the slot entrance will be measured using the floating metal ring mounted near the inner diameter at the entrance to the slot. This measurement will yield the high and low frequency asymmetry factors. Langmuir probes will be used to measure the electron temperature and plasma density in the main and peripheral plasmas. The rf discharge voltage, current, and power will be measured using an existing Z-scan probe, and the dc bias voltage will be measured. If needed, an rf B-field probe will be used to examine the rf currents and magnetic fields near the walls, which may play a role in discharge maintenance. Light measurements and corresponding measurements with Langmuir probes will be used to investigate the instabilities. These measurements of breakdown and maintenance will be compared to model predictions and used to guide improvements in the model.

VI. CONCLUSIONS AND FUTURE WORK

We have developed theories to describe plasma diffusion from a capacitive discharge into a slot, and the breakdown and maintenance of plasma in the grounded slot and a grounded peripheral pumping region. In Sec. II, we showed that the main dishcharge plasma diffuses into the slot between the quartz confinement rings, forming a "finger" of plasma of width w_{po}. We found that $w_{po} \propto g$, the slot thickness, and weakly depends on the other discharge parameters. For nominal dishcharge conditions with $g = 0.5$ cm, a 1 cm finger of plasma forms in the slot.

In Sec. III, we modified the standard one-dimensional global model for capacitive discharges to treat discharge maintenance, incorporating the additional physics required at low rf driving voltages, including

both rf and dc parts to the sheath and resistive voltage drops across the sheaths and bulk plasma. We compared the maintenance condition from the modified model with measurements for a conventional 13.56 MHz discharge, finding reasonable agreement.

In Sec. IV, we examined the two-dimensional effects present in a confined dual frequency geometry, including wave propagation, radial rf current flows, and capacitive voltage drops across the width of the quartz confinement rings. We incorporated these into the one-dimensional model, and used it to determine the maintenance conditions for the slot and peripheral plasmas in the confined geometry at 27.12 MHz. We found that, depending on the discharge condtions, either maintenance of the slot plasma or the periphery plasma determines the loss of confinement in the system.

In Sec. V, we described initial measurements from an experiment designed to study the confinement of plasma in a dual frequency system similar to that used for commercial application. We found that a significant hysteresis exists in the loss of confinement and ignition of the peripheral and slot plasmas, and we discovered instabilities associated with the loss of confinement in both the kilohertz and hertz frequency range. We believe that the theory qualitatively explains the observations made in our experiment and in a commercial reactor of a similar configuration, of transitions between conditions in which the plasma is confined to the central discharge, and conditions in which plasma also exists in the peripheral grounded regions.

To obtain good quantitative agreement between theory and experiment a number of subtle effects must be included in the model. Many of these have already been incorporated, while other effects will be included as the experimental and theoretical comparisons are made. Although the experiment is in operation and initial results obtained, a detailed experimental exploration of parameters is still in its initial stages. The experimental observations of hysteresis in the confinement transitions with changing power, and the observation of instabilities in the kilohertz and hertz ranges, may be understood qualitatively from the model, but must be confirmed by including time variation of parameters in the model, that allow us to predict the effects quantitatively.

The initial experiments have been carried out with a single slot thickness and a single 27.12 MHz high frequency source. The ongoing comparisons will at first continue to use the single source, while varying the gap spacing, which will be a good test of the basic theory. When the agreement between theory and experiment is deemed to be satisfactory, a low frequency bias source will be added to describe a complete dual frequency system. The low frequency bias has already been incorporated into the model, and the experiments may uncover additional complications when two frequencies are imployed, which will then be investigated.

We gratefully acknowledge the support provided by the Lam Research Corporation, the State of California MICRO Program, National Science Foundation Grant ECS-0139956, and a UC Discovery Grant from the Industry-University Cooperative Research Program (IUCRP).

REFERENCES

1. M.A. Lieberman and A.J. Lichtenberg, *Principles of Plasma Discharges and Materials Processing,* (Wiley, New York, 1994) .
2. P. Chabert, J.L. Raimbault, J.M. Rax, and M.A. Lieberman, *Phys. Plasmas* **11** 1775 (2004).
3. V.A. Lisovskii, *Tech. Phys.* **43** 526 (1998).
4. L. Rhode, *Ann. Physik* **5** 569 (1932).
5. G.M. Pateiuk, *Sov. Phys. JETP* **3** 14 (1956).
6. G. Francis, *Ionization Phenomena in Gases,* (Butterworths, London, 1960) Chapter 4.
7. V. Lisovsky and V.D. Yegorenkov, *J. Phys. D: Appl. Phys.* **32** 2645 (1999).
8. V.A. Godyak, R.B. Piejak, and B.M. Alexandrovich, *IEEE Trans. Plasma Sci.* **19** 660 (1991).
9. W.P. Allis and D.J. Rose, *Phys. Rev.* **93** 84 (1954).
10. S.C. Brown, *Basic Data of Plasma Physics,* (Wiley, New York, 1959) .
11. H.B. Smith, C. Charles, and R.W. Boswell, *Phys. Plasmas* **10** 875 (2003).
12. A.J. Hatch and H.B. Williams, *J. Appl. Phys.* **25** 417 (1954).
13. M.A. Lieberman, J.P. Booth, P. Chabert, J.M. Rax, and M.M. Turner, *Plasma Sources Sci. Technol.* **11** 283 (2002).